Article

Chemical Understanding of a Non-IPR Metallofullerene: Stabilization of Encaged Metals on Fused-Pentagon Bonds in La@C

Xing Lu, Hidefumi Nikawa, Tsukasa Nakahodo, Takahiro Tsuchiya, Midori O. Ishitsuka, Yutaka Maeda, Takeshi Akasaka, Makoto Toki, Hiroshi Sawa, Zdenek Slanina, Naomi Mizorogi, and Shigeru Nagase

J. Am. Chem. Soc., **2008**, 130 (28), 9129-9136 • DOI: 10.1021/ja8019577 • Publication Date (Web): 21 June 2008

J|A|C|S
ARTICLES

Published on Web 06/21/2008

Chemical Understanding of a Non-IPR Metallofullerene: Stabilization of Encaged Metals on Fused-Pentagon Bonds in $La_2@C_{72}$

Xing Lu,[†] Hidefumi Nikawa,[†] Tsukasa Nakahodo,[†] Takahiro Tsuchiya,[†] Midori O. Ishitsuka,[†] Yutaka Maeda,[‡] Takeshi Akasaka,*[,†] Makoto Toki,[§] Hiroshi Sawa,[§] Zdenek Slanina,[†] Naomi Mizorogi,[||] and Shigeru Nagase*[,||]

Center for Tsukuba Advanced Research Alliance, University of Tsukuba, Tsukuba, Ibaraki 305-8577, Japan, Department of Chemistry, Tokyo Gakugei University, Tokyo 184-8501, Japan, Institute of Materials Structure Science, High-Energy Accelerator Research Organization, Tsukuba 305-0801, Japan, and Department of Theoretical and Computational Molecular Science, Institute for Molecular Science, Okazaki 444-8585, Japan

Received March 17, 2008; E-mail: akasaka@tara.tsukuba.ac.jp

Abstract: Fullerenes violating the isolated pentagon rule (IPR) are only obtained in the form of their derivatives. Since the [5,5]-bond carbons are highly reactive, they are easily attacked by reagents to release the bond strains. Non-IPR endohedral metallofullerenes, however, still have unsaturated sp^2 carbons at the [5,5] bond junctions, which allow their chemical properties to be probed. In this work, $La_2@C_{72}$ was chosen as a representative non-IPR metallofullerene, since it has been experimentally proposed to have either the #10611 or #10958 non-IPR cage structure (*J. Am. Chem. Soc.* **2003**, *125*, 7782), while theoretical calculations have suggested that the #10611 cage is more stable (*J. Phys. Chem. A* **2006**, *110*, 2231). $La_2@C_{72}$ was modified by photolytic reaction with the carbene reagent 2-adamantane-2,3-[3H]-diazirine. Six isomers of adamantylidene monoadducts were isolated and characterized using various kinds of measurements, including high-performance liquid chromatography, matrix-assisted laser desorption ionization mass spectrometry, UV−vis−near-infrared spectroscopy, cyclic voltammetry, differential-pulse voltammetry, ^{13}C NMR spectroscopy, and single-crystal X-ray diffraction. Electronic spectra and electrochemical studies revealed that the essential electronic structures of $La_2@C_{72}$ are retained in the six isomers and the adamantylidene group acts as a weak electron-donating group toward $La_2@C_{72}$. X-ray structural results unambiguously elucidated that $La_2@C_{72}$ has the #10611 chiral cage (i.e., D_2 symmetry) with two pairs of fused pentagons at each pole of the cage and that the two La atoms reside close to the two fused-pentagon pairs. On the basis of these results and theoretical calculations, it is concluded that the fused-pentagon sites are very reactive toward carbene but that the carbons forming the [5,5] junctions are less reactive than the adjacent ones; this confirms that these carbons interact strongly with the encaged metals and thus are stabilized by them.

1. Introduction

Fullerenes are closed-carbon-cage molecules consisting of exactly 12 pentagons and a variable number of hexagons.[1–3] For example, the experimentally most abundant fullerene, I_h-symmetric C_{60}, contains 12 pentagons and 20 hexagons. The arrangement of these five-membered and six-membered carbon rings is controlled by the well-known isolated pentagon rule (IPR),[4] which states that each pentagon on a fullerene cage should be surrounded by hexagons in a stable fullerene isomer. The [5,5]-bond carbons of fused pentagons bear greater bond strains and are accordingly very reactive toward other reagents, thus prohibiting either structural stability or solubility of non-IPR species.[5] Since its formulation, the IPR has proved in practice to be valuable in unraveling the structures of higher fullerenes, as it has been strictly obeyed by all pure-carbon fullerenes isolated to date.[1,2] However, non-IPR fullerenes are always attractive not only because of their unique structures, which contain fused pentagons, but also because of their unusual properties resulting from the high curvatures around the adjacent pentagons.[6,7] As a result, great efforts to seek fullerene isomers with non-IPR structures have been made. Recently, several successful examples have been achieved, showing that non-

[†] University of Tsukuba.
[‡] Tokyo Gakugei University.
[§] High-Energy Accelerator Research Organization.
[||] Institute for Molecular Science.

(1) *Fullerenes: Chemistry, Physics, and Technology*; Kadish, K., and Ruoff, R. Eds.; John Wiley & Sons: New York, 2000.
(2) *An Atlas of Fullerenes*; Fowler, P. W., and Manolopolous, D. E. Eds.; Clarendon Press: Oxford, 1995.
(3) *Endofullerenes: A New Family of Carbon Clusters*; Akasaka, T., and Nagase, S. Eds.; Kluwer: Dordrecht, The Netherlands, 2002.
(4) Kroto, H. W. *Nature* **1987**, *329*, 529.
(5) Schmaltz, T. G.; Seitz, W. A.; Klein, D. J.; Hite, G. E. *J. Am. Chem. Soc.* **1988**, *110*, 1113.
(6) Curry, J. D. *J. Exp. Biol.* **1999**, *202*, 3285.
(7) Kamat, S.; Su, X.; Ballarini, R.; Heuer, A. H. *Nature* **2000**, *405*, 1036.

Scheme 1. Photoreaction of $La_2@C_{72}$ with **1**

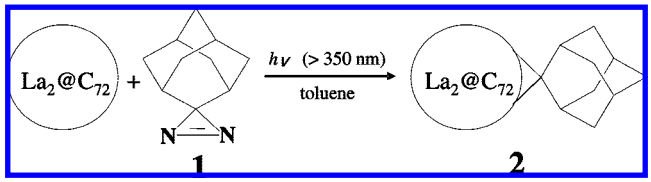

IPR fullerenes with fused pentagons can be stabilized by either exohedral derivatization or endohedral metal-doping. [8–21]

Upon exohedral derivatization, the hybridization state of the carbons forming the fused-pentagon bonds is changed from sp^2 to sp^3 by the addition of hydrogen or hetero groups; thus, the bond strain is considerably mitigated, and stable derivatives become obtainable.[8–10] For example, $C_{50}Cl_{10}$ and $C_{64}H_4$ were synthesized by introducing extra reagents into the DC arc-discharge reactor, and then these compounds were successfully isolated and structurally characterized. The results disclosed that $C_{50}Cl_{10}$ contains five pairs of fused pentagons along its cage equator while $C_{64}H_4$ bears a set of triply fused pentagons.[8,9] Interestingly, it was found that the substituents (Cl or H) were added exclusively to the carbons of [5,5] bond junctions, revealing that the reactivity of abutted-pentagon carbons is much higher than that of carbons at other sites of the carbon cage as a result of the high surface curvatures. Furthermore, replacement of the Cl groups of $C_{50}Cl_{10}$ with methanol via solvolysis reactions indicated that the highly curved surfaces of the fused-pentagon regions were still active for further chemical transformations.[8] In addition, two other examples of substituted non-IPR fullerenes, $C_{58}F_{17}CF_3$ and $C_{58}F_{18}$, were successfully obtained upon fluorination of C_{60}. These compounds contain one heptagon surrounded by fused pentagons and hexagons. In these two derivatives, the pentagon−pentagon carbons and nearby carbons were functionalized with −F or $-CF_3$ groups to release the bond strains, which also implies high reactivity of fused-pentagon sites.[10]

Meanwhile, the inner cavities of fullerenes have been found to be able to encapsulate metal atoms or clusters, thus generating a new class of materials with novel structures and properties as well as interesting applications, some of which are not expected for empty fullerenes.[3] These new materials, which are commonly called endohedral metallofullerenes (EMFs), have become a promising subject in materials science.[3] As a result of charge transfer from the encapsulated metal species to the carbon cage, some otherwise unstable fullerene cages, including several non-IPR ones, were synthesized and isolated.[11–15] $Sc_2@C_{66}$ and $Sc_3N@C_{68}$ were the first reported examples of fullerene cages violating the IPR restriction (as there is no IPR-satisfying isomer[11,12] for either C_{66} or C_{68}). Later, $Sc_2C_2@C_{68}$, $Tb_3N@C_{84}$, and $Sc_3N@C_{70}$ were also shown to bear fused-pentagon structures.[13–15] All of these reported species have fused-pentagon pairs whose number is equal to the number of encapsulated metal atoms, except for $Tb_3N@C_{84}$, which has three encapsulated Tb atoms but only one fused-pentagon pair.[14] Thus, it has been believed that the fused-pentagon pairs in non-IPR EMFs are stabilized by electron transfer from the encapsulated metals to the carbon cage. Actually, both experimental results and theoretical calculations have indicated that the encaged metals are associated with the fused-pentagon pairs in non-IPR EMFs, but more direct experimental proof is still lacking.[11–18] Furthermore, unlike the exohedrally derivatized non-IPR fullerenes, non-IPR EMFs still bear unsaturated sp^2 carbons at the [5,5] bond junctions, and thus, it is of special interest to elucidate the properties and chemical reactivities of the fused pentagons. However, little is known about the properties of non-IPR fullerenes and non-IPR EMFs.

Recently, a missing-caged metallofullerene, $La@C_{72}$, was isolated in the form of its dichlorobenzene derivative. Structural analysis confirmed that $La@C_{72}$ has a non-IPR carbon cage with only one pair of fused pentagons and that the dichlorophenyl group is not connected to the reactive carbons of the [5,5] junction but instead is singly bonded to a carbon adjacent to the [5,5] junction on the fused-pentagon rings.[19] This is the only example to date of an exohedral derivative of a non-IPR EMF. However, since pristine $La@C_{72}$ is unavailable because of its poor solubility in common organic solvents, the chemical properties of intact [5,5]-bond carbons of non-IPR fullerenes and non-IPR EMFs still remain unknown.

Fortunately, another missing-caged metallofullerene, $La_2@C_{72}$, is an isolable species that may possess a non-IPR cage (#10611 or #10958) with two pairs of fused pentagons, as proposed by Shinohara and co-workers[20,21] on the basis of the observation of a ^{13}C NMR spectrum containing 18 lines of equal intensity. Theoretical calculations suggested that $La_2@C_{72}$ prefers to take the D_2-symmetric #10611 cage, since it is energetically more stable.[20,16] Subsequent calculations by Popov and Dunsch[17] also confirmed that $La_2@C_{72}$ has the #10611 cage, while the #10958 cage is more suitable for $Sc_3N@C_{72}$. However, unambiguous experimental results on the definite structure of $La_2@C_{72}$ are still lacking.

In this work, $La_2@C_{72}$ was allowed to react with 2-adamantane-2,3-[3H]-diaziridine (AdN_2, **1**) via photolysis in order to characterize the molecular structure of $La_2@C_{72}$ exactly and, more importantly, to obtain valuable information about the chemical reactivity of sp^2 carbons at fused-pentagon junctions,. Six monoadduct isomers were isolated and characterized, and the three most abundant ones were structurally determined using single-crystal X-ray diffraction (XRD) as well as ^{13}C NMR spectroscopy.

(8) Xie, S.; Gao, F.; Lu, X.; Huang, R.; Wang, C.; Zhang, X.; Liu, M.; Deng, S.; Zheng, L. *Science* **2004**, *304*, 699.
(9) Wang, C.; Shi, Z.; Wan, L.; Lu, X.; Dunsch, L.; Shu, C.; Tang, Y.; Shinohara, H. *J. Am. Chem. Soc.* **2006**, *128*, 6605.
(10) Troshin, P. A.; Avent, A. G.; Darwish, A. D.; Martsinovich, M.; Abdul-Sada, A. K.; Street, J. M.; Taylor, R. *Science* **2005**, *309*, 278.
(11) Wang, C.; Kai, T.; Tomiyama, T.; Yoshida, T.; Kobayashi, Y.; Nishibori, E.; Takata, M.; Sakata, M.; Shinohara, H. *Nature* **2000**, *408*, 426.
(12) Stevenson, S.; Fowler, P. W.; Heine, T.; Duchamp, J. C.; Rice, G.; Glass, T.; Harich, K.; Hajdu, E.; Bible, R.; Dorn, H. C. *Nature* **2000**, *408*, 428.
(13) Shi, Z.; Xu, X.; Wang, C.; Lu, X.; Shinohara, H. *Angew. Chem., Int. Ed.* **2006**, *45*, 2107.
(14) Beavers, C. M.; Zuo, T.; Duchamp, J. C.; Harich, K.; Dorn, H. C.; Olmstead, M. M.; Balch, A. L. *J. Am. Chem. Soc.* **2006**, *128*, 11352.
(15) Yang, S.; Popov, A. A.; Dunsch, L. *Angew. Chem., Int. Ed.* **2007**, *46*, 1256.
(16) Slanina, Z.; Chen, Z.; Schleyer, P. R.; Uhlik, F.; Lu, X.; Nagase, S. *J. Phys. Chem. A* **2006**, *110*, 2231.
(17) Popov, A. A.; Dunsch, L. *J. Am. Chem. Soc.* **2007**, *129*, 11835.
(18) Park, S. S.; Liu, D.; Hagelberg, F. *J. Phys. Chem. A* **2005**, *109*, 8865.
(19) Wakahara, T.; Nikawa, H.; Kikuchi, T.; Nakahodo, T.; Rahman, G. M. A.; Tsuchiya, T.; Maeda, Y.; Akasaka, T.; Yoza, K.; Horn, E.; Yamamoto, K.; Mizorogi, N.; Slanina, Z.; Nagase, S. *J. Am. Chem. Soc.* **2006**, *128*, 14228.
(20) Kato, H.; Taninaka, A.; Sugai, T.; Shinohara, H. *J. Am. Chem. Soc.* **2003**, *125*, 7782.
(21) Taninaka, A.; Kato, H.; Shino, K.; Sugai, T.; Heike, S.; Terada, Y.; Suwa, Y.; Hashizume, T.; Shinohara, H. *Jpn. J. Appl. Phys.* **2003**, *44*, 3226.

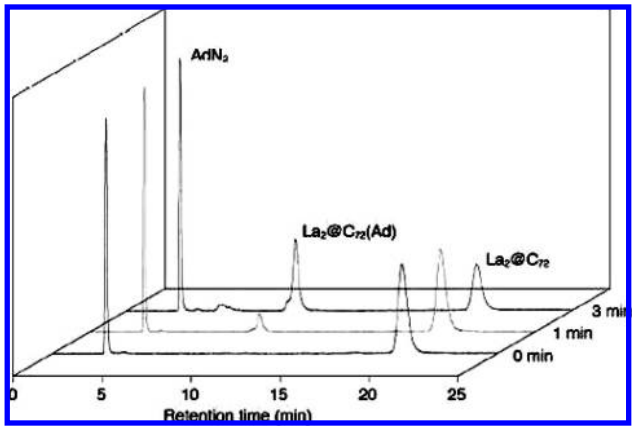

Figure 1. HPLC profiles of a reaction mixture containing $La_2@C_{72}$ and **1**.

2. Experimental Section

A Pyrex tube containing a mixture of $La_2@C_{72}$ and **1** in dry toluene was photoirradiated ($\lambda > 350$ nm) with a high-pressure mercury-arc lamp at room temperature (Scheme 1). High-performance liquid chromatography (HPLC) was used to monitor the reaction, and the profiles are shown in Figure 1. Before irradiation, the starting materials **1** and $La_2@C_{72}$ gave strong peaks at retention times of 5 and 22 min, respectively. After irradiation for 1 min, a new peak appeared at 13 min, which was ascribed to monoadducts of $La_2@C_{72}$(Ad) (Ad = adamantylidene carbene),**2**, as identified from mass spectrometric results. After irradiation for 3 min, additional formation of monoadducts and consumption of pristine $La_2@C_{72}$ as well as generation of small amounts of bisadducts (at a retention time of 10 min) were detected, and the reaction was terminated. The conversion was estimated to be 60% on the basis of the HPLC results. Subsequent separation using three-stage recycling HPLC gave six monoadduct isomers, **2a**, **2b**, **2c**, **2d**, **2e**, and **2f**, with relative abundances of 8, 9, 40, 36, 4, and 3%, respectively, as calculated from their HPLC peak areas. Thus, **2c** and **2d** are the two major isomers, and the other four are the minor ones. The isomers were further characterized using various methods. Additional experimental details and the HPLC separation profiles are given in the Supporting Information.

3. Results and Discussion

3.1. Composition and Stability of $La_2@C_{72}$(Ad). Matrix-assisted laser desorption ionization−time-of-flight (MALDI−TOF) mass spectroscopic results provided direct evidence for the formation of 1:1 adducts. The mass spectra of **2a**−**2f** were almost identical to each other, so only the spectrum of **2a** is shown in Figure 2 as a representative (the others are given in the Supporting Information). As Figure 2 clearly shows, only one molecular-ion peak [at *m*/*z* 1276 ascribed to $La_2@C_{72}$(Ad)] was observed, and no peaks due to bis- or multiadducts were detected. The observed isotopic distribution of the ion peak agreed well with the calculated results for $La_2@C_{72}(C_{10}H_{14})$. The absence of the $La_2@C_{72}$ peak is worth noting, because previously reported derivatives of metallofullerenes always lost the addends during mass spectrometric measurements;[22–28] the present result thus suggests that $La_2@C_{72}$(Ad) isomers are very stable with respect to laser decomposition.

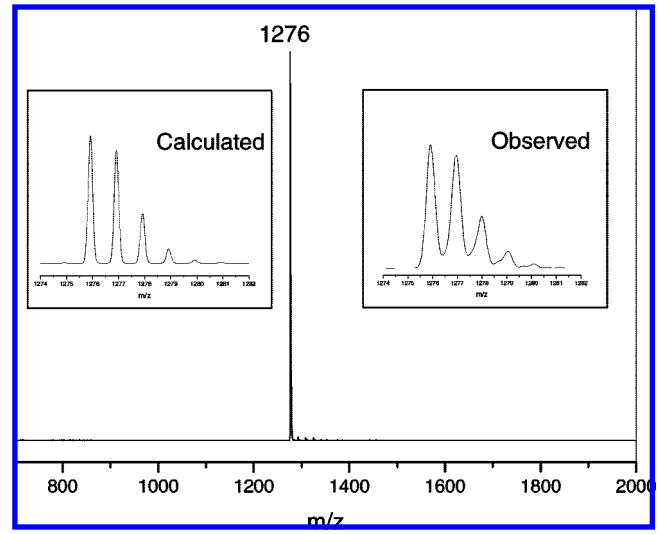

Figure 2. MALDI-TOF mass spectrum of **2a** in negative-ion mode; the left and right insets show calculated and observed isotopic distributions, respectively.

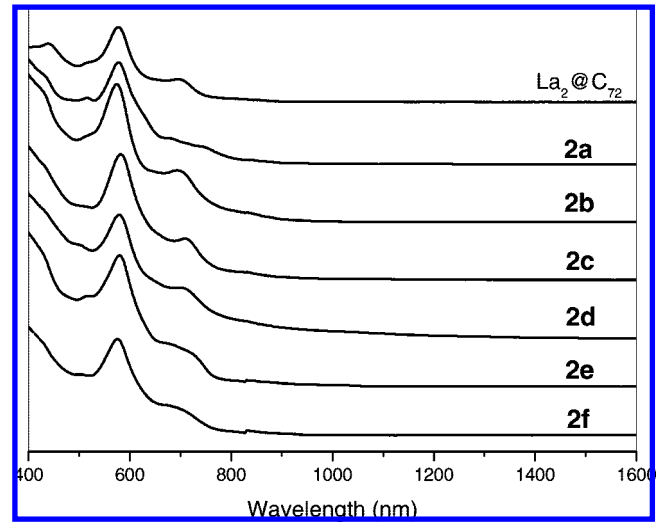

Figure 3. Vis−NIR spectra of $La_2@C_{72}$ and **2a**−**2f**.

In addition, it was found that **2a**−**2f** are also stable in solution. For example, solutions of **2a**−**2f** kept for 4 months under an argon atmosphere gave HPLC traces identical to those of the newly isolated products, indicating that all six isomers are thermodynamically stable products.

3.2. Electronic Structure. UV−vis−near-infrared (NIR) spectrometry is commonly used to characterize the electronic structures of fullerenes, EMFs, and their derivatives. As shown in Figure 3, the vis−NIR spectrum of pristine $La_2@C_{72}$ displays a featured curve consisting of three major absorptions at 510, 580, and 710 nm and a weak band at 810 nm. The onset is observed at 950 nm, showing that $La_2@C_{72}$ has a large band gap (~1.3 eV), which should account for its isolability.[29] After

(22) Akasaka, T.; Kato, T.; Kobayashi, K.; Nagase, S.; Yamamoto, K.; Funasaka, H.; Takahashi, T. *Nature* **1995**, *374*, 600.
(23) Iezzi, E. B.; Duchamp, J. C.; Harich, K.; Glass, T. E.; Lee, H. M.; Olmstead, M. M.; Balch, A. L.; Dorn, H. C. *J. Am. Chem. Soc.* **2002**, *124*, 524.
(24) Lu, X.; Xu, J.; He, X.; Shi, Z.; Gu, Z. *Chem. Mater.* **2004**, *16*, 953.
(25) Yamada, M.; Feng, L.; Wakahara, T.; Maeda, Y.; Lian, Y.; Kako, M.; Akasaka, T.; Kato, T.; Kobayashi, K.; Nagase, S. *J. Phys. Chem. B* **2005**, *109*, 6049.
(26) Cardona, C. M.; Kitaygorodskiy, A.; Echegoyen, L. *J. Am. Chem. Soc.* **2005**, *127*, 10448.
(27) Li, X.; Fan, L.; Liu, D.; Sung, H.; Williams, I.; Yang, S.; Tan, K.; Lu, X. *J. Am. Chem. Soc.* **2007**, *129*, 10636.
(28) Stevenson, S.; Stephen, R. R.; Amos, T. M.; Cadorette, V. R.; Reid, J. E.; Phillips, J. P. *J. Am. Chem. Soc.* **2005**, *127*, 12776.

Table 1. Redox Potentials (V) of $La_2@C_{72}$ and **2a**−**2f**[a]

compound	$^{ox}E_2$	$^{ox}E_1$	$^{red}E_1$	$^{red}E_2$
$La_2@C_{72}$	+0.75[b]	+0.24	−0.68	−1.92
2a	+0.66	+0.15	−0.68	−1.99[b]
2b	+0.64	+0.12	−0.80	−
2c	+0.67	+0.15	−0.76	−2.00[b]
2d	+0.60	+0.10	−0.79	−2.06[b]
2e	+0.48	+0.02	−0.82	−2.07[b]
2f	+0.67	+0.12	−0.82	−2.05[b]

[a] Half-cell potentials unless otherwise noted. Values are relative to the ferrocenium/ferrocene couple and were obtained at a Pt working electrode in a 1,2-dichlorobenzene solution containing 0.1 M $(n\text{-Bu})_4NPF_6$. [b] Irreversible values obtained using DPV.

modification with **1**, these features are essentially retained in the monoadducts **2a**−**2f** with only very slight alterations, indicating that the π-electron system of $La_2@C_{72}$ is not significantly changed by addition of the Ad group. According to published results, EMF derivatives with ring-opened structures, such as the Bingel−Hirsch adducts of $Y_3N@C_{80}$[30] and $La@C_{82}$,[31] prefer to keep the electronic features of their precursors, while EMF derivatives bearing closed-cage structures show significant alterations of the UV−vis spectra. For example, the UV−vis spectra of the Bingel−Hirsch derivatives of $Sc_3N@C_{78}$, which have closed-cage structures, differed significantly from that of pristine $Sc_3N@C_{78}$.[32] Accordingly, the similarities in the UV−vis−NIR spectra of **2a**−**2f** and $La_2@C_{72}$ suggest that the six isomers should have open-cage structures, as in the case of $La@C_{82}$(Ad).[33,34]

Furthermore, cyclic voltammetry (CV) and differential-pulse voltammetry (DPV) measurements were also performed on $La_2@C_{72}$ and **2a**−**2f** in order to characterize their electrochemical behaviors. The CV curve of $La_2@C_{72}$ (Figure S5 in the Supporting Information) contained two reductive and two oxidative waves in the range from +1.0 to −2.2 V; **2a**−**2f** displayed similar curves (Figure S9 in the Supporting Information), with the corresponding redox potentials cathodically shifted. As summarized in Table 1, the redox potentials of **2a**−**2f** were 0.05−0.15V more negative than those of $La_2@C_{72}$, indicating that the Ad group has a mild electron-donating ability toward $La_2@C_{72}$.

3.3. Geometric Structure. To obtain structural information, a ^{13}C NMR measurement was first performed on the most abundant isomer, **2c** (Figure S10 in the Supporting Information). The total of 82 ^{13}C NMR lines indicated that **2c** has C_1 symmetry. The 10 lines in the sp^3 region (27−47 ppm) were ascribed to the carbons in the Ad unit, while the signals at 102 and 110 ppm were attributed to the two cage carbons making bonds with Ad. The remaining 69 distinct lines (one doublet due to coincident overlapping) in the range 124−158 ppm were due to the sp^2 carbons of the C_{72} cage. If we assume that

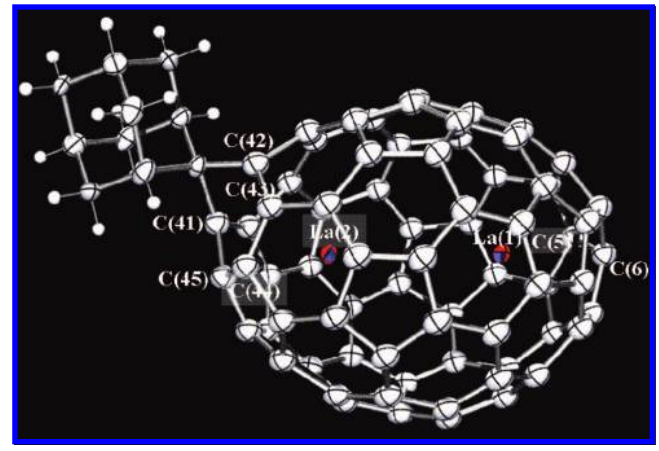

Figure 4. ORTEP drawing of **2b**, showing thermal ellipsoids at the 50% probability level. The 1,2-dichlorobenzene molecules have been omitted for clarity. The two [5,5] bond junctions in $La_2@C_{72}$ (#10611) are C(5)−C(6) and C(44)−C(45).

$La_2@C_{72}$ has a non-IPR cage (either #10611 or #10958, both of which have D_2 symmetry), as reported by Shinohara and coworkers,[20] the observation of 82 ^{13}C NMR lines suggests that the addition of Ad does not occur at the reactive [5,5] bond junctions because fewer ^{13}C NMR signals would be observable in that case.

On the basis of the X-ray structural determination (see below), we calculated the ^{13}C NMR spectrum of **2c** using density functional theory at the B3LYP level[35,36] [the LANL2DZ basis set[37] with the effective core potential for La and the 6−311G* basis for C and H (B3LYP/6−311G*∼dz treatment) was used, while the geometry was optimized at the B3LYP/3−21G∼dz level] with inclusion of the shift calibration,[38] as implemented in the Gaussian 03 program.[39] The computed spectrum was in good agreement with the observed one (Figure S10 in the Supporting Information).

To unambiguously disclose the structure of $La_2@C_{72}$ and its monoadducts, formation of single crystals of **2a**−**2f** was attempted. Fortunately, good single crystals of three most abundant isomers (i.e., **2b**, **2c**, and **2d**) suitable for X-ray structural analysis were obtained, and their molecular structures were clearly resolved.

The structure of the minor isomer **2b** (with a relative abundance of 9%) was determined first and is shown in Figure 4. It is evident that $La_2@C_{72}$ has two pairs of fused pentagons, one at each of the two poles of the molecule; C(5)−C(6) and C(44)−C(45) are the two [5,5] bond junctions. Detailed analyses disclosed that $La_2@C_{72}$ takes the chiral cage #10611 with D_2 symmetry, excluding the possibility of cage #10958 and confirming the results of the theoretical calculations.[16,17,20]

It is worth mentioning that for the C_{72} fullerene, there is only one IPR-satisfying isomer, which has D_{6d} symmetry.[2] However, C_{72} has been called a "missing fullerene" because it has never been isolated.[40] Theoretical calculations on C_{72} and $Ca@C_{72}$ suggested that non-IPR cages of C_{72} are more

(29) Diener, M. D.; Alford, J. M. *Nature* **1998**, *393*, 668.
(30) Lukoyanova, O.; Cardonar, C. M.; Rivera, J.; Lugo-Morales, L. Z.; Chancellor, C. J.; Olmstead, M. M.; Rodriguez-Fortea, A.; Poblet, J. M.; Balch, A. L.; Echegoyen, L. *J. Am. Chem. Soc.* **2007**, *129*, 10423.
(31) Feng, L.; Tsuchiya, T.; Wakahara, T.; Nakahodo, T.; Piao, Q.; Maeda, Y.; Akasaka, T.; Kato, T.; Yoza, K.; Horn, E.; Mizorogi, N.; Nagase, S. *J. Am. Chem. Soc.* **2006**, *128*, 5990.
(32) Cai, T.; Xu, L.; Gibson, H. W.; Dorn, H. C.; Chancellor, C. J.; Olmstead, M. M.; Balch, A. L. *J. Am. Chem. Soc.* **2007**, *129*, 10795.
(33) Maeda, Y.; et al. *J. Am. Chem. Soc.* **2004**, *126*, 6858.
(34) Akasaka, T.; Kono, T.; Matsunaga, Y.; Wakahara, T.; Nakahodo, T.; Ishitsuka, M. O.; Maeda, Y.; Tsuchiya, T.; Kato, T.; Liu, M. T. H.; Mizorogi, N.; Slanina, Z.; Nagase, S. *J. Phys. Chem. A* **2008**, *112*, 1294.
(35) Becke, A. D. *J. Chem. Phys.* **1993**, *98*, 5648.
(36) Lee, C.; Yang, W.; Parr, R. G. *Phys. Rev. B* **1988**, *37*, 785.
(37) Hay, P. J.; Wadt, W. R. *J. Chem. Phys.* **1985**, *82*, 299.
(38) Sun, G. Y.; Kertesz, M. *J. Phys. Chem. A* **2000**, *104*, 7398.
(39) Frisch, M. J.; et al. GAUSSIAN 03, revision C.01; Gaussian, Inc.: Wallingford, CT, 2004.
(40) Wan, T. S. M.; Zhang, H.-W.; Nakane, T.; Xu., Z.; Inakuma, M.; Shinohara, H.; Kobayashi, K.; Nagase, S. *J. Am. Chem. Soc.* **1998**, *120*, 6806.

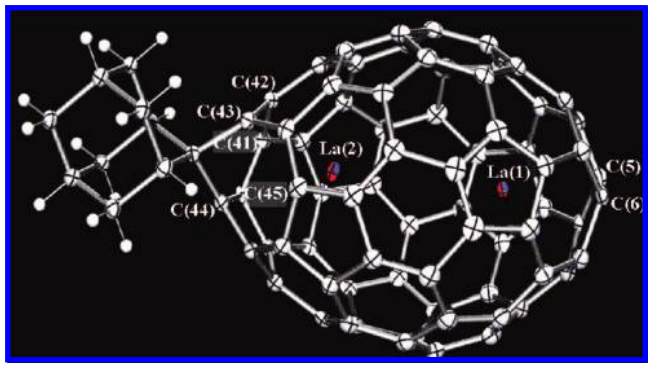

Figure 5. ORTEP drawing of **2c**, showing thermal ellipsoids at the 50% probability level. The 1,2-dichlorobenzene molecules have been omitted for clarity. The two [5,5] bond junctions of $La_2@C_{72}$ (#10611) are C(5)−C(6) and C(44)−C(45).

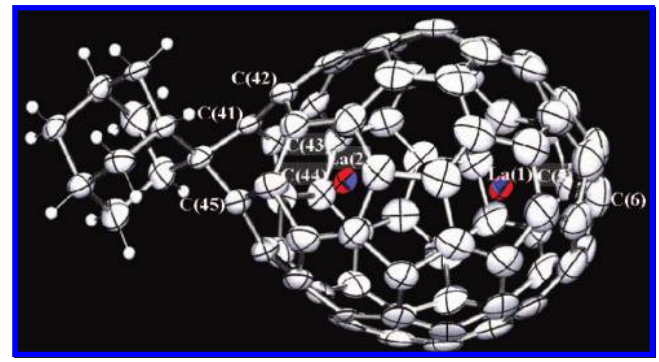

Figure 6. ORTEP drawing of **2d**, showing thermal ellipsoids at the 50% probability level. The 1,2-dichlorobenzene molecules have been omitted for clarity. The two [5,5] bond junctions of $La_2@C_{72}$ (#10611) are C(5)−C(6) and C(44)−C(45).

stable than the IPR-satisfying one.[41,42] Recently, it was found that $La@C_{72}$ has a non-IPR cage structure with one pair of fused pentagons.[19] Our new X-ray structural assignment of $La_2@C_{72}$ is notable since it adds $La_2@C_{72}$ to the C_{72}-based missing fullerene family as a new non-IPR member with two pairs of fused pentagons.

After noting this wider context, we now return to the molecular structure of **2b**. As shown in Figure 4, the addition of Ad occurred at C(41)−C(42), a [5,6] bond junction shared by one of the fused pentagons and an adjacent hexagon and located a bit far from the [5,5] bond junction C(44)−C(45) of pristine $La_2@C_{72}$. An open-cage structure for **2b** was confirmed by the C(41)−C(42) distance of 2.096 Å, which accounts for the essential preservation of the electronic structure of pristine $La_2@C_{72}$. The two La atoms reside at the two poles of the C_{72} cage, with the La(1)−La(2) axis perpendicular to the two [5,5] bond junctions. The distance between La(1) and La(2) is 4.171 Å, indicative of a strong repulsion between them. The La(1) atom, which is far from the Ad group, sits close to the [5,5] bond junction C(5)−C(6), with La(1)−C(5) and La(1)−C(6) distances of 2.511 and 2.472 Å, respectively. For the La(2) atom, which is close to the Ad unit, the La(2)−C(44) and La(2)−C(45) distances of 2.537 Å and 2.475 Å, respectively, are comparable to the La(1)−C(5) and La(1)−C(6) distances, indicating that the two La atoms prefer to coordinate with the [5,5]-junction bonds. The bond distances of the two [5,5] junctions [1.440 and 1.453 Å for C(5)−C(6) and C(44)−C(45), respectively] are similar to each other, showing that the addition of Ad to the C(41)−C(42) bond had little effect on the character of the C(44)−C(45) bond in **2b** even though a bond in one of the fused pentagons was broken.

The X-ray structure of the most abundant isomer, **2c**, was also obtained. As Figure 5 clearly shows, the addition of the Ad group also took place at a [5,6] bond junction, C(43)−C(44), but this one is located next to the [5,5] junction C(44)−C(45). The C(43)−C(44) distance is 2.104 Å, indicative of an open-cage structure. This agrees with the conclusions from the UV−vis results. The two La atoms reside at the poles of the C_{72} cage, and the La(1)−La(2) distance is 4.178 Å. The La−La unit is again oriented with its axis turned across the two [5,5] bond junctions. The La(1) atom far from the Ad group is placed closer to the carbons of its nearby [5,5] bond than is the La(2) atom near the Ad unit. The La(1)−C(5) distance of 2.501 Å differs little from the La(1)−C(6) distance of 2.495 Å, evidencing strong interactions between the encaged metal and the [5,5] bond junction; the La(2)−C(44) and La(2)−C(45) distances (2.851Å and 2.604 Å, respectively) are somewhat longer than the corresponding La(1) distances. In contrast, the of La(2)−C(41), La(2)−C(42), and La(2)−C(43) distances (2.388, 2.278, and 2.573 Å, respectively) are considerably shorter. These indicate that La(2) has moved from the position of sitting on the [5,5] bond to the location of the broken five-membered ring, where a larger cavity is provided. In addition, the C(44)−C(45) bond distance of 1.465 Å is longer than that (1.408 Å) for the [5,5] junction C(5)−C(6), indicating that the double-bond character of C(44)−C(45) is weakened by the addition of Ad in **2c**.

Finally, the molecular structure of the other major isomer, **2d**, was also determined from the X-ray data and is presented in Figure 6. The Ad addition still occurs at a [5,6] bond junction [C(41)−C(45)] that is adjacent to the [5,5] bond junction C(44)−C(45). The long C(41)−C(45) distance of 2.023 Å suggests that **2d** also has an open-cage structure. The La(1)−La(2) distance of 4.175 Å is similar to the corresponding values for **2b** and **2c**. The La(1) atom far from the Ad group is still located close to the [5,5] bond junction C(5)−C(6), with La(1)−C(5) and La(1)−C(6) distances of 2.477 Å and 2.483 Å, respectively, again showing strong interactions between the encaged metal and the [5,5] bond junction. For the La(2) atom close to the Ad unit, the La(2)−C(44) and La(2)−C(45) distances (2.508 Å and 2.706 Å, respectively) are somewhat longer. La(2) is located closer to C(43), with a La(2)−C(43) distance of 2.464 Å, suggesting that La(2) has moved to the cavity of the broken pentagon. Furthermore, the C(5)−C(6) bond distance of 1.386 Å is significantly shorter than the C(44)−C(45) distance of 1.535 Å, confirming that the double-bond character of the C(44)−C(45) bond junction in **2d** was also weakened by the ring-opening in one of its fused pentagons.

Selected bond distances from the X-ray results for **2b**, **2c**, and **2d** are listed in Table 2. In general, the hemisphere on which Ad is not attached seems to remain unchanged in **2b**−**2d**, as indicated by the C(5)−C(6), La(1)−C(5), and La(1)−C(6) distances. However, the structures of the other side of the molecule change considerably. In **2b**, the [5,5] bond distance C(44)−C(45) and the distances from La(2) to C(44) and C(45) are comparable to the corresponding ones in the unchanged

(41) Kobayashi, K.; Nagase, S.; Yoshida, M.; Osawa, E. *J. Am. Chem. Soc.* **1997**, *119*, 12693.
(42) Slanina, Z.; Kobayashi, K.; Nagase, S. *Chem. Phys. Lett.* **2003**, *372*, 810.

Table 2. Selected Bond Distances (Å) in the Single-Crystal X-ray Structures of **2b**, **2c**, and **2d**

isomer	La(1)−La(2)	C(5)−C(6)	La(1)−C(5)	La(1)−C(6)	C(44)−C(45)	La(2)−C(44)	La(2)−C(45)
2b	4.171	1.440	2.511	2.472	1.453	2.537	2.475
2c	4.178	1.408	2.501	2.495	1.465	2.851	2.604
2d	4.175	1.386	2.477	2.483	1.535	2.508	2.706

hemisphere, indicating that the Ad addition to a bond far from the [5,5] junction has little effect on the strong interaction between the encaged metal and the fused-pentagon bond. In both **2c** and **2d**, the C(44)−C(45) bond distance is considerably longer than the [5,5] bond distances in the other hemisphere, and La(2) also moves from a position sitting on the [5,5] bond to the cavity of the broken pentagon. These results suggest that the breaking of a bond closer to the [5,5] junction has a greater effect on the position of the adjacent encaged metal[43] and confirm that the two La atoms in pristine $La_2@C_{72}$ are coordinated strongly with the [5,5] bonds.

As is obvious from the X-ray data, no major isomer was produced by the addition of Ad to the [5,5] bond junctions. This is somewhat surprising, since H or Cl groups add exclusively to the fused-pentagon bonds in non-IPR fullerenes, as found for $C_{64}H_4$ and $C_{50}Cl_{10}$.[8,9] To provide deeper insight into the chemical properties of $La_2@C_{72}$ and the structures of **2a**−**2f**, theoretical calculations were performed as described below.

3.4. Reactivity of Fused-Pentagon Carbons in $La_2@C_{72}$. The D_2-symmetric C_{72} cage coded #10611 has 18 different types of carbons, as evidenced by the observation of 18 ^{13}C NMR lines. Interestingly, the four carbons in the two [5,5] bonds are equivalent. Relief of local strain on each carbon of the fullerene is one of the main driving forces for exohedral additions. The pyramidalization angles, defined as π-orbital axis vector (POAV) values ($\theta_{\pi\pi} - 90°$), provide a valuable index of local strains.[44] First, we computed POAV values[44] and Mulliken charge densities for the 18 types of carbons of $La_2@C_{72}$, and the results are shown in Figure 7a. As expected, the curvatures in the fused-pentagon areas are obviously higher than those in other areas, as evidenced by the large POAV values. In addition, high charge densities were found for the fused-pentagons and nearby carbons, indicative of strong metal−carbon-cage interactions. Therefore, only those carbon atoms having both high charge densities and large POAV values must be considered.

Figure 7b presents a clearer view of one fused-pentagon pair in $La_2@C_{72}$ (#10611), in which the encaged La atoms have been omitted, only the carbons forming and linking to the fused pentagons are shown, and equivalent counterparts are marked with the same letter and color. As Figure 7b shows, the e-type carbons constituting the [5,5]-junction have the greatest POAV value, and the three other types of carbons in the fused-pentagon pair (the c, f, and b types) have relatively large POAV values. The other types of carbons (a, d, and g), which connect to the fused-pentagon part, have relatively small POAV values. However, the highest charge density is found for the d-type carbons, which are not part of the fused pentagons, and the b-, c-, f-, g-, and a-type carbons have relatively high charge densities. Meanwhile, the [5,5]-junction carbons (e type) have the lowest charge density. It has been verified that Ad acts as

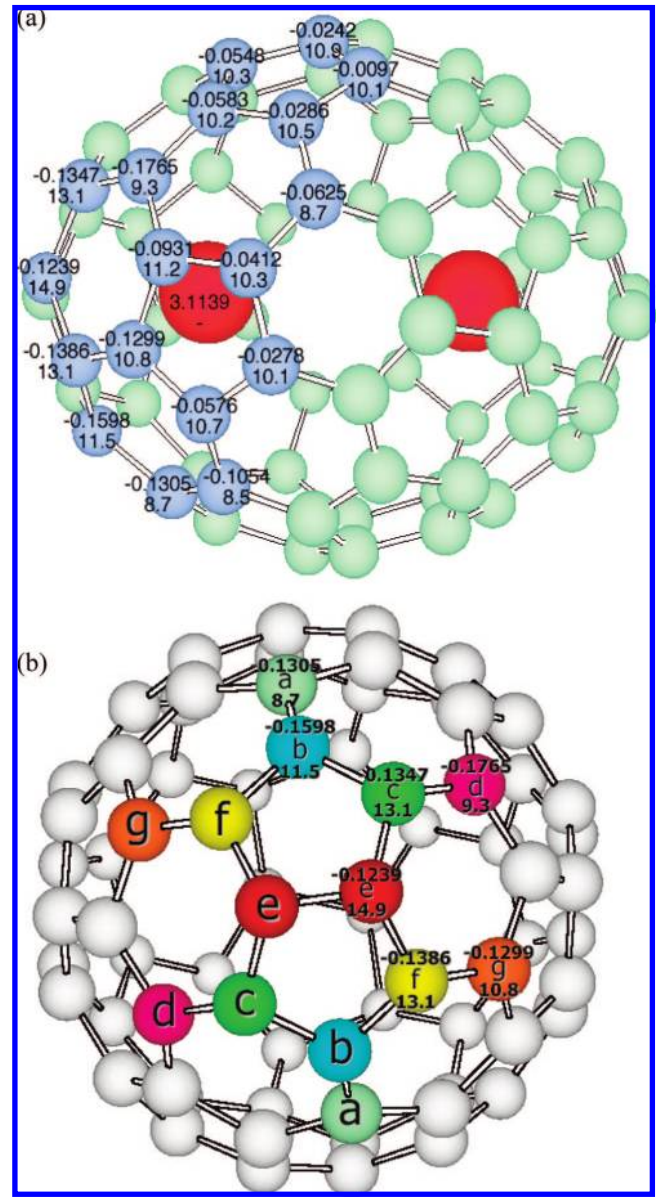

Figure 7. (a) Side view of $La_2@C_{72}$, in which the calculated charge densities (upper numbers) and POAV values (lower numbers) are indicated for the 18 types of carbons. (b) Top view of $La_2@C_{72}$ without the La atoms, showing only the carbons forming and linking to the fused-pentagon pairs (matching colors and letters indicate equivalent carbon atoms).

an electrophile when it reacts with $La@C_{82}$.[33,34] Obviously, Ad tends to attack the electron-rich c- and f-type carbons in the fused-pentagon regions of $La_2@C_{72}$ instead of the e-type carbons, though the latter have the highest POAV value.

As confirmed by single-crystal X-ray analysis, one major isomer (**2c**) was generated by the addition of Ad to c- and e-type sites (Figure 5), while the other (**2d**) was formed via Ad addition to e- and f-type carbons (Figure 6). This is perfectly consistent with the facts that c- and f-type carbons have almost identical charge densities and POAV values and that **2c** and **2d** had nearly equal abundances (40 and 36%, respectively). Since one minor isomer (**2b**) was confirmed to be formed via addition of Ad to b- and f-type carbons (Figure 4), it is highly likely that one of the remaining three minor isomers (probably **2a**) was formed

(43) Yamada, M.; Someya, C.; Wakahara, T.; Tsuchiya, T.; Maeda, Y.; Akasaka, T.; Yoza, K.; Horn, E.; Liu, M. T. H.; Mizorogi, N.; Nagase, S. *J. Am. Chem. Soc.* **2008**, *130*, 1171.

(44) Haddon, R. C. *Science* **1993**, *261*, 1545.

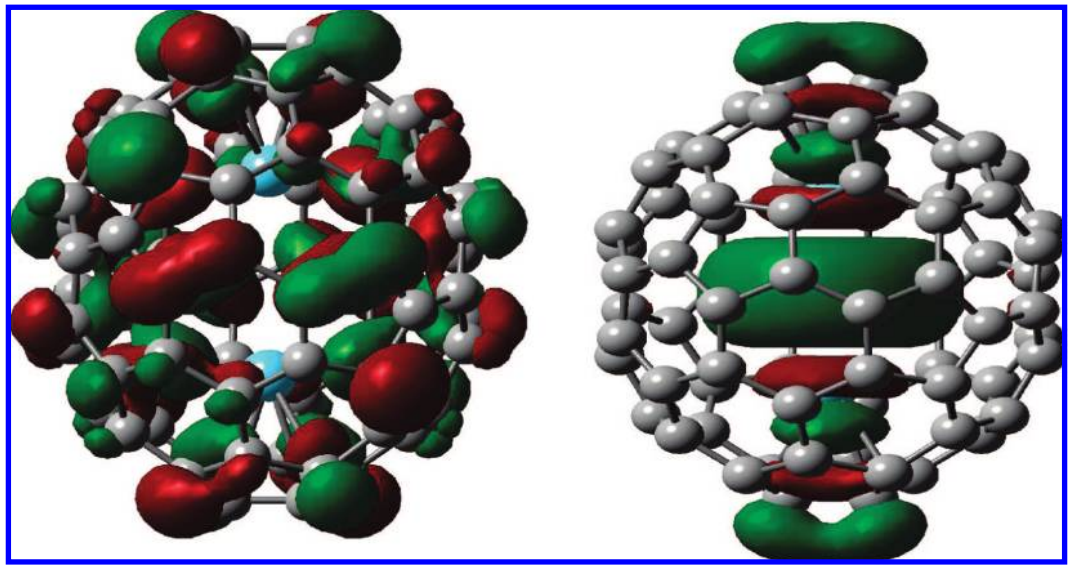

Figure 8. (left) HOMO and (right) LUMO of $La_2@C_{72}$.

by addition to b- and c-type carbons.[45] Obviously, no major isomer of $La_2@C_{72}$(Ad) was formed via Ad addition to the [5,5] junctions (e−e junctions), and thus it is reasonable to conclude that c- and f-type carbons are more reactive toward Ad than e-type ones. Accordingly, because of the high reactivities of the c- and f-type carbons, c−d and f−g bond junctions are the most probable addition sites for the remaining two minor isomers. These conclusions are also in good agreement with the HOMO/LUMO distributions for $La_2@C_{72}$ (#10611). As shown in Figure 8, the HOMO is mainly localized on the carbon cage but does not contain the e-type carbons, indicating that these carbons are less reactive toward the Ad electrophile. However, the LUMO is completely localized on the e-type carbons and the encaged metals, and accordingly, it is predicted that e-type carbons remain reactive toward nucleophiles.

The electrophilic Ad group shows a high selectivity toward $La@C_{82}$.[33,34] It selectively attacks one of the electron-rich strained carbons of the six-membered ring closest to the encaged La atom, forming only one monoadduct isomer even though there are 24 nonequivalent cage carbons in $La@C_{82}$ (C_{2v}).[33] This result showed that the encaged metal has a directional effect controlling the reactivity of the cage carbons via metal−cage charge transfer. For the non-IPR EMF $La_2@C_{72}$, six monoadduct isomers were obtained, indicating that the active sites in $La_2@C_{72}$ are somehow less selective toward **1** than those in $La@C_{82}$. However, our results have shown that Ad selectively attacks a c- or f-type carbon and then connects to one of the three adjacent carbons, resulting in the formation of six isomers with open-cage structures. Thus, we conclude that the c- and f-type carbons adjacent to the [5,5] junction are more reactive than the e-type carbons that form the [5,5] junction.

Similar results were also found[19] for the derivatives of the non-IPR EMF $La@C_{72}$: the dichlorophenyl radical attacks the carbons adjacent to the [5,5]-bond carbons instead of the [5,5]-bond carbons themselves, confirming that the adjacent carbons are more reactive. This manner of stabilization is obviously different from that involving chemical substitution of the [5,5]-junction carbons in C_{50} and C_{64}, in which hydrogen or chlorine exclusively attacks the [5,5]-bond carbons to release the bond strains. Obviously, the difference results from the fact that the [5,5] bond junctions are coordinated with the encapsulated metals and thus are stabilized. In fact, non-IPR fullerenes have never been isolated without derivatization, though some have been detected using mass spectroscopy. However, non-IPR EMFs are always found in carbon soot, and some have been isolated, as discussed in the Introduction.[8–20] These results suggest that non-IPR EMFs are clearly more stable than the corresponding empty non-IPR fullerenes. Herein we have presented direct proof of the stabilization of [5,5] junctions by encaged metals from the point of view of chemistry, which provides a deeper understanding of the structures, properties, and formation mechanisms of non-IPR fullerenes and non-IPR EMFs.

4. Conclusion

$La_2@C_{72}$ was successfully derivatized using **1**, and six monoadduct isomers were isolated and characterized. X-ray structural analysis of the three most abundant isomers (**2b**, **2c**, and **2d**) unambiguously disclosed that $La_2@C_{72}$ has a non-IPR chiral cage coded #10611 with two pairs of fused pentagons, one at each end of the molecule. The addition of Ad to $La_2@C_{72}$ mainly took place at the fused pentagons. The calculated charge densities and POAV values of the carbons of $La_2@C_{72}$ together with the relative abundances of **2a**−**2f** disclosed that no adduct was generated via the addition of Ad to the [5,5] bond junctions. Accordingly, we conclude that the carbons of the fused-pentagon pairs are very reactive because of the high surface curvature but that the [5,5]-bond carbons are not as reactive as those in empty non-IPR fullerenes, thereby proving that the [5,5] bond junctions in $La_2@C_{72}$ are stabilized by the encaged metals. Interestingly, the carbons adjacent to the [5,5] bond junctions were found to be the most active sites. Our results not only add a new member to the non-IPR fullerene family but also (and more importantly) provide valuable clues to the mechanism of stabilization of [5,5] bond junctions by the encaged metals in non-IPR metallofullerenes. These clues should help increase our

(45) C(41), C(42), and C(43) in Figures 4–6 correspond to f-, b-, and c-type carbons, respectively, of pristine $La_2@C_{72}$, as shown in Figure 7b, while C(5), C(6), C(44), and C(45) are e-type carbons.

understanding of the chemical reactivities, properties, and broadening future applications of non-IPR fullerenes and non-IPR EMFs.

Acknowledgment. H.N. thanks the Japan Society for the Promotion of Science (JSPS) for the Research Fellowship for Young Scientists. We thank T. Wakahara for interesting discussions. This work was supported in part by a Grant-in-Aid, the 21st Century COE Program, the Nanotechnology Support Project, the Next Generation Super Computing Project (Nanoscience Project), and Scientific Research on Priority Area from the Ministry of Education, Culture, Sports, Science, and Technology of Japan as well as by a grant from the Kurata Memorial Hitachi Science and Technology Foundation.

Supporting Information Available: Complete citations for refs 33 and 39, experimental details, spectroscopic data for $La_2@C_{72}$ and $La_2@C_{72}$(Ad) isomers, and X-ray crystallographic details and CIF files for **2b**, **2c**, and **2d**. This material is available free of charge via the Internet at http://pubs.acs.org.

JA8019577